

APPLIED PHYSICS

A polarization-induced 2D hole gas in undoped gallium nitride quantum wells

Reet Chaudhuri^{1*}, Samuel James Bader², Zhen Chen², David A. Muller^{2,4}, Huili Grace Xing^{1,3,4}, Debdeep Jena^{1,3,4}

A high-conductivity two-dimensional (2D) hole gas, analogous to the ubiquitous 2D electron gas, is desirable in nitride semiconductors for wide-bandgap p-channel transistors. We report the observation of a polarization-induced high-density 2D hole gas in epitaxially grown gallium nitride on aluminium nitride and show that such hole gases can form without acceptor dopants. The measured high 2D hole gas densities of about 5×10^{13} per square centimeters remain unchanged down to cryogenic temperatures and allow some of the lowest p-type sheet resistances among all wide-bandgap semiconductors. The observed results provide a probe for studying the valence band structure and transport properties of wide-bandgap nitride interfaces.

The high-conductivity quantum-confined two-dimensional (2D) electron gases (2DEGs) at the interface of AlGaIn/GaN semiconductor heterostructures, discovered in the mid-1990s (1), did not require the presence of chemical dopants. The origin of the 2DEG was tracked down to the existence of broken inversion symmetry along the [0001] axis of gallium nitride (GaN), combined with the high polarity of the metal-nitrogen bond in GaN and aluminium nitride (AlN) (2, 3). These properties, as well as the tensile epitaxial strain of AlN on GaN, lead to the presence of spontaneous P_{sp} and piezoelectric P_{pz} polarization in AlN/GaN heterostructures (4). The polarization difference $[(P_{sp}^{AlN} + P_{pz}^{AlN}) - P_{sp}^{GaN}] \cdot \hat{n} = \sigma_{\pi}$ constitutes a net-positive fixed-polarization sheet charge. This charge, with the potential barrier of a large conduction band offset, induces a 2DEG at such a heterojunction, without any chemical doping. The carrier concentration that can be induced by the polar discontinuity far exceeds what is achievable in the bulk with chemical doping or at junctions with modulation doping. Such robust polarization-induced 2DEGs in Al(Ga)N/GaN heterojunctions have been investigated for the past two decades and contributed to several applications, such as ultrafast unipolar transistors and sensors (5, 6).

However, the p-type analog of the undoped polarization-induced 2DEG—the undoped 2D hole gas (2DHG)—has remained elusive. Although low-density 2D and 3D hole gases have been previously inferred in nitride heterojunctions in several reports (7–16), they have been either modulation Mg-doped heterostructures or structures

in which both mobile electrons and holes are present. Substantial advances in energy-efficient wide-bandgap electronics are expected for GaN/AlN-based high-voltage complementary switches (17), if a high-conductivity undoped 2DHG can be generated.

In contrast to the 2DEG structure, if a thin layer of metal-polar GaN is grown on a relaxed AlN substrate, the net interface polarization difference, $[(P_{sp}^{GaN} + P_{pz}^{GaN}) - P_{sp}^{AlN}] \cdot \hat{n} = \sigma_{\pi}$, is negative in sign and should induce holes. The valence band offset of AlN and GaN confines the 2DHG, as schematically shown in the energy band diagram of Fig. 1A, a self-consistent solution of a multiband $k \cdot p$ and Poisson equations (18). A mobile 2D hole gas of sheet density roughly equal to the fixed interface polarization charge $\sigma_{\pi} \sim 5 \times 10^{13} \text{ cm}^{-2}$ is expected to form at the heterojunction, depending on the thickness of the GaN layer.

The schematic of GaN/AlN layer structures, which we grew using molecular beam epitaxy (MBE), is shown in Fig. 1B (19). We observed a sharp heterojunction between wurtzite GaN and AlN, with the GaN layer pseudomorphically strained (Fig. 1, C and D) (20). Further structural and chemical details are shown in Fig. 2. The as-grown surface has a smooth morphology, with clearly resolved atomic steps (Fig. 2A). The fringes and multiple peaks of the x-ray diffraction spectrum (Fig. 2B) indicate a smooth, uniform heterostructure over the entire millimeter-scale beam size. This was further corroborated by the large-area scanning transmission electron microscopy (STEM) images in fig. S1. A reciprocal-space x-ray map indicates that the GaN epitaxial layer is fully, biaxially, compressively strained (by 2.4%) to the underlying AlN layer (Fig. 2C). Thus, the heterostructure is structurally and chemically in a form that should exhibit the undoped polarization-induced 2DHG (Figs. 1 and 2), and the transport studies discussed next indicate that this is the case.

The layer structure of three samples is shown in Fig. 3A: Sample A is an undoped ~13-nm GaN

layer on AlN. Sample B is identical to A, except that the top 10 nm of GaN are doped with Mg to lock the Fermi level to valence band edge separation, screening the 2DHG from variations of the surface potential. For comparison with conventional acceptor doping, a thick Mg-doped GaN (sample C) was also measured. The temperature-dependent Hall-effect transport properties of the three samples are shown in Fig. 3, A to C, measured from 300 to 10 K. The mobile charge density $n_s = IB/qV_H$ is obtained from the Hall voltage V_H that develops upon driving a current I through the 2D hole gas in a magnetic field B perpendicular to its plane. The Hall voltage results from the Lorentz force $F = q(v \times B)$, which drives holes in a direction opposite to electrons, leading to a positive sign. The carrier mobility $\mu_p = 1/qn_s R_s$ is obtained from the measured sheet resistance R_s . The positive slope of the Hall resistance (V_H/I) versus magnetic field and positive Hall-coefficient sign for all samples in this study ensured that we were studying and comparing only holes.

The resistivity of the Mg-doped bulk GaN control sample C increases sharply with the lowering of temperature from ~40 kilohms/square at 300 K to 2 megohms/square at ~180 K (Fig. 3A). This increase in resistivity is almost entirely caused by the ~100× decrease of the thermally generated mobile hole density, which freezes out with an activation energy $E_A \sim 170$ meV (Fig. 3B). We observed a dramatically different behavior for the undoped heterostructure sample A and the Mg-doped heterostructure B. They showed metallic behavior, with the resistivity decreasing with decreasing temperature, which is a signature of a degenerate 2D hole gas.

The resistivity of heterostructure A decreased from ~6.0 kilohm/square at 300 K to ~1 kilohm/square at 10 K, and the resistivity of heterostructure B decreased from ~8.0 kilohm/square at 300 K to ~2 kilohm/square at 20 K (Fig. 3A). Because the hole densities measured in samples A and B are nearly independent of temperature (Fig. 3B), all the change in the resistivity was caused by an increase in the hole mobility as the temperature was lowered. The high hole sheet densities measured are similar for the doped and undoped heterostructures in samples A and B because the integrated acceptor sheet density in sample B is only $\sim 5 \times 10^{12} \text{ cm}^{-2}$, which is about an order of magnitude lower than the measured mobile hole gas density. This direct measurement, without any other parallel 2DEG or 3D hole channels, thus points to the presence of a high-density polarization-induced 2D hole gas in the undoped heterojunction. Contactless wafer-scale sheet resistivity measurements shown in fig. S3 confirm the presence of the hole gas in the undoped structures, corroborating that holes are polarization-induced and exist at the heterojunction independent of whether metal layers are deposited on the surface.

The mobility of the 2D hole gas in the undoped heterostructure increases from ~25 $\text{cm}^2/\text{V}\cdot\text{s}$ at 300 K to ~190 $\text{cm}^2/\text{V}\cdot\text{s}$ at 10 K and in the doped heterostructure increases from ~20 $\text{cm}^2/\text{V}\cdot\text{s}$ at

¹School of Electrical and Computer Engineering, Cornell University, Ithaca, NY 14853, USA. ²School of Applied and Engineering Physics, Cornell University, Ithaca, NY 14853, USA. ³Department of Materials Science and Engineering, Cornell University, Ithaca, NY 14853, USA. ⁴Kavli Institute at Cornell for Nanoscale Science, Cornell University, Ithaca, NY 14853, USA.

*Corresponding author. Email: rtc77@cornell.edu

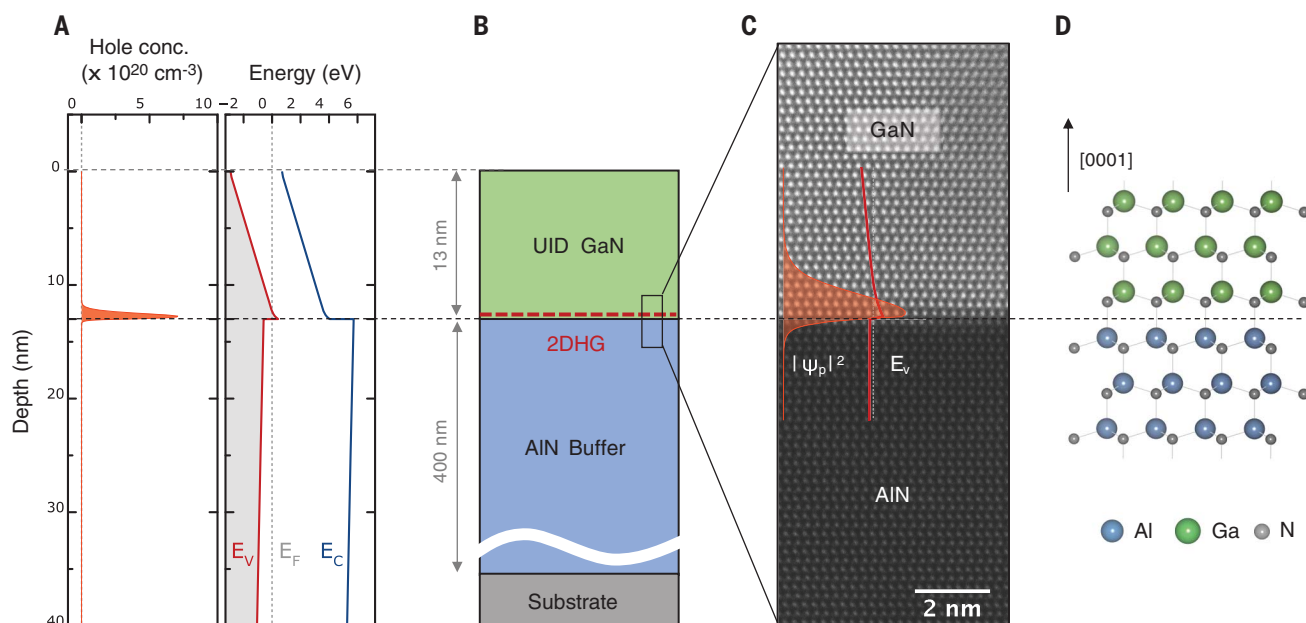


Fig. 1. Epitaxially grown GaN/AlN heterostructures. (A) Energy-band diagram of a 13-nm undoped GaN on AlN heterostructure, showing the formation of a quantum well in the valence band and the high-density of confined holes accumulated at the GaN/AlN interface. (B) Schematic of the epitaxially grown layer structure. (C) High-

resolution STEM image showing the metal-polar wurtzite crystalline lattice of the heterointerface. The valence band edge, and probability density of the holes from (A) are overlaid on the interface. (D) Schematic of the metal-polar GaN/AlN heterointerface (20), corresponding to the STEM image in (C).

300 K to $\sim 120 \text{ cm}^2/\text{V}\cdot\text{s}$ at 20 K, an increase of $\sim 6\times$ to $7\times$ (Fig. 3C). The variation of the measured 2D hole gas mobility with temperature is expected to be strongly influenced by acoustic phonon scattering (27), in addition to the polar optical phonon scattering that dominates in most polar compound semiconductors. Although the hole mobilities do not saturate at $\sim 10 \text{ K}$, an extrapolation points to values in the range of $\sim 200 \text{ cm}^2/\text{V}\cdot\text{s}$. Because the 2D hole gas density survives to cryogenic temperatures, magneto-transport studies can be used to directly access and probe the nature of the valence band of GaN.

We observed the 2DHGs in multiple samples similar to samples A and B with reproducible properties (table S1). As further evidence for the polarization-induced origin of the 2D hole gas, the variation of the density of the 2D hole gas with the thickness of the GaN layer is shown in fig. S2, marking a well-defined critical thickness. This is the exact dual of what is observed in the undoped polarization-induced Al(Ga)N/GaN 2DEG (22) and provides a valuable degree of freedom for p-channel transistor design.

How do the observed polarization-induced 2D hole gases in the undoped and doped GaN/AlN heterostructures compare with those reported in nitride semiconductors and in general with hole gases across various semiconductor material systems? The 2DHG densities of $\sim 5 \times 10^{13} \text{ cm}^{-2}$ measured in this work (listed in table S1) are near the expected polarization difference and much higher than previously reported 2DHG densities in nitride semiconductors (Fig. 4A) (8–15). The hole densities are among the highest among all

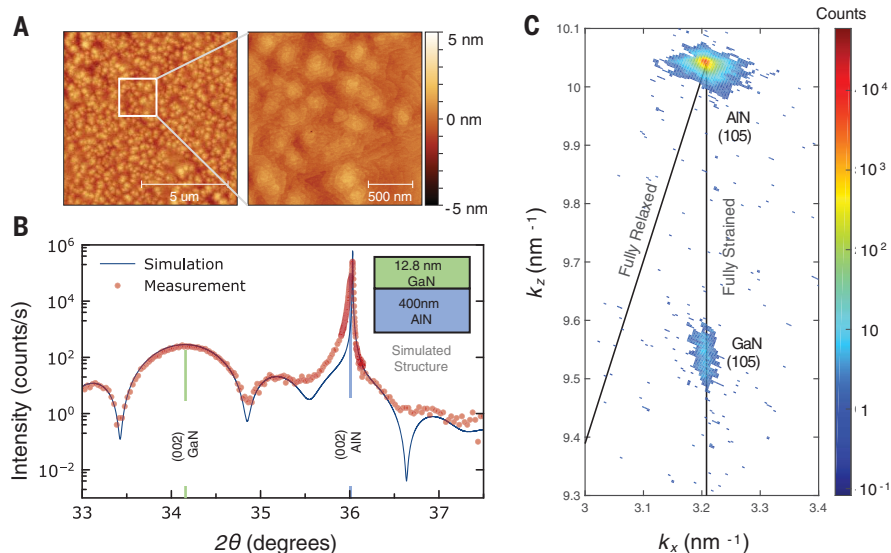


Fig. 2. Structural properties of the MBE-grown GaN/AlN heterostructures. (A) Atomic force microscopy (AFM) scans of the as-grown surface. The root mean square roughnesses are ~ 0.69 and $\sim 0.46 \text{ nm}$ for the 10 and $2 \mu\text{m}$ scans, respectively. (B) X-ray diffraction (XRD) 2θ scan across the symmetric (002) reflection and the simulated data (19), confirming the targeted thicknesses and sharp interfaces. (C) Reciprocal space map scan of the asymmetric (105) reflections of GaN and AlN shows that the 13-nm GaN layer is fully strained to the AlN layer.

semiconductor systems, including GaAs/AlGaAs (23, 24), $\text{SrTiO}_3/\text{LaAlO}_3$ (25), surface-conducting diamond (26–30), heterostructures with Ge channels (31–35), Si inversion channels (36), and heterostructures with GaSb channels (37–39), as

shown in Fig. 4B. The high 2D hole density in the nitride leads to some of the lowest sheet resistances, despite lower hole mobilities.

The 2DHG mobilities in the wide-bandgap nitrides are not comparatively high because of

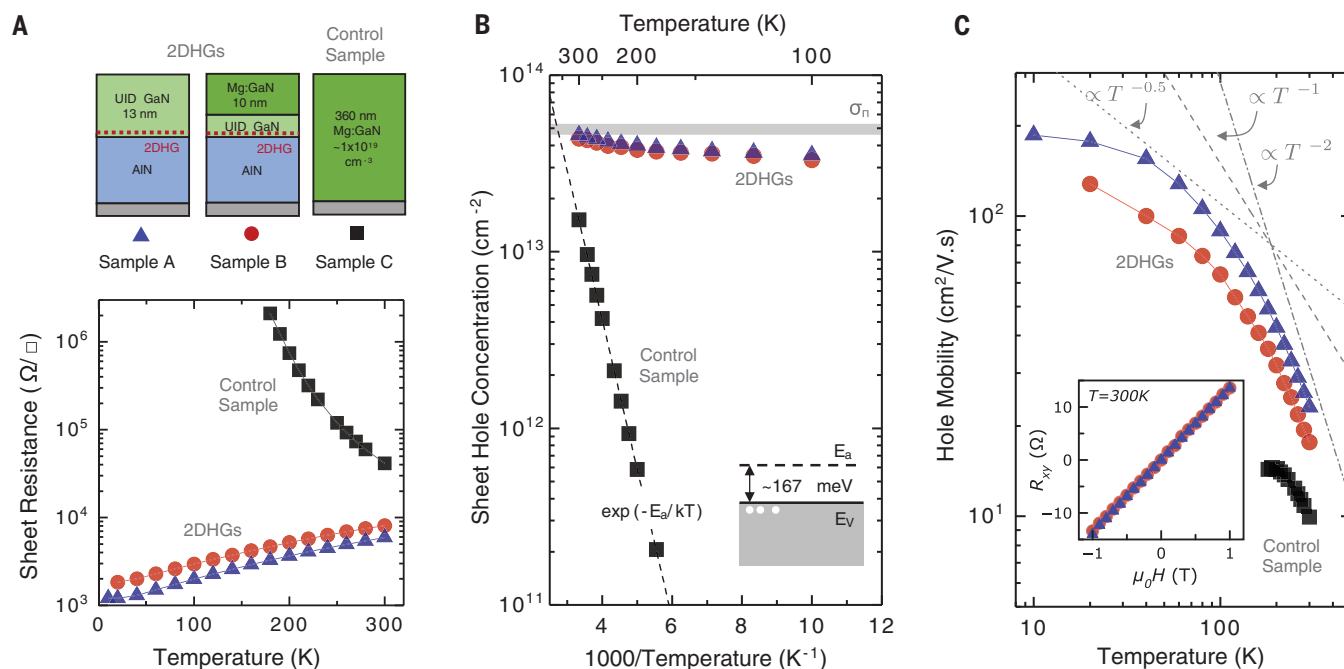


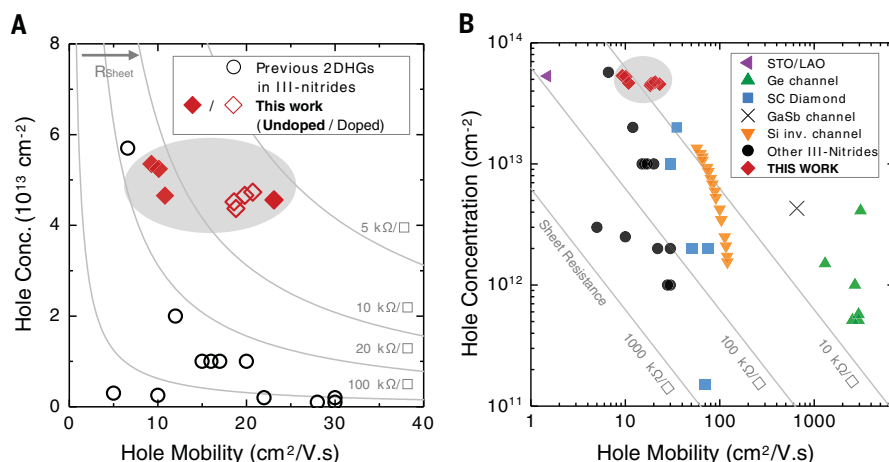
Fig. 3. Temperature-dependent magnetotransport measurements.

Shown are the data from 300 to 10 K at 1 T magnetic field of 2DHG samples A and B, along with a Mg-doped GaN control sample C. **(A)** The 2DHG samples A and B exhibit a metallic behavior of decreasing sheet resistance with decreasing temperature, whereas the control sample C is insulating in behavior, becoming too resistive below $\sim 180 \text{ K}$ for measurement. **(B)** The measured mobile hole concentrations over a range of temperatures in samples A, B, and C. In the Mg-doped

GaN (sample C), holes freeze out below 180 K. The density in the 2DHG of samples A and B show almost no change in the hole concentration down to cryogenic temperatures. **(C)** The measured hole mobilities in samples A, B, and C for a range of temperatures. The 2DHG in samples A and B show higher mobilities than that of C. (Inset) Hall resistance versus magnetic field measured at room temperature indicates a positive Hall coefficient (holes) in both samples A and B.

Fig. 4. Comparison of room-temperature transport properties of 2D hole gases with prior work.

(A) Comparison with previously reported 2DHGs in nitride heterostructures (8–14) (open symbols indicate Mg-typed doping). The doped as well as undoped structures reported in this work have much higher hole densities and decent mobilities, enabling record high p-type conductivity of $\sim 6 \text{ k}\Omega/\text{square}$. **(B)** Comparing across other semiconductor material systems such as oxides $\text{SrTiO}_3/\text{LaAlO}_3$ (25), surface conducting diamond (26–29), Ge channels (31–35), Si inversion channels (36), and GaSb channels (37), this work has the highest room-temperature hole density and the highest conductivities among wide-bandgap semiconductors (III-nitrides, oxides, and diamond), the latter of which is critical for high-performing lateral power devices.



the high effective mass of both heavy and light holes in GaN (40). However, a large bandgap means that the high 2D hole gas densities can be modulated effectively with a gate through field effect because the semiconductor intrinsically is capable of sustaining much larger electric fields. Because of the fundamentally different origin of the 2DHG in the nitrides, this form of doping is expected to scale down to the individual unit cells of the semiconductor crystal and not be

affected by random dopant fluctuations in case of Mg-doping in GaN.

Mg acceptor doping was a key breakthrough in making GaN photonics feasible (41); however, the experimental observation of the polarization-induced undoped 2D hole gas in this work shows that Mg acceptor doping is not compulsory for the generation of holes in nitride semiconductors. The internal broken-symmetry-induced polarization fields have enough strength to provide holes

of very high densities, with several potential scientific and technological applications.

REFERENCES AND NOTES

1. M. A. Khan, J. N. Kuznia, J. M. Van Hove, N. Pan, J. Carter, *Appl. Phys. Lett.* **60**, 3027–3029 (1992).
2. O. Ambacher et al., *J. Appl. Phys.* **85**, 3222–3233 (1999).
3. F. Bernardini, V. Fiorentini, D. Vanderbilt, *Phys. Rev. B Condens. Matter* **56**, R10024–R10027 (1997).
4. C. Wood, D. Jena, Eds., *Polarization Effects in Semiconductors: From Ab Initio Theory to Device Applications* (Springer, 2007).

5. S. J. Pearton *et al.*, *J. Phys. Condens. Matter* **16**, R961–R994 (2004).
6. U. K. Mishra, L. Shen, T. E. Kazior, Y.-F. Wu, *Proc. IEEE* **96**, 287–305 (2008).
7. T. Zimmermann *et al.*, *IEEE Electron Device Lett.* **25**, 450–452 (2004).
8. R. Chu, Y. Cao, M. Chen, R. Li, D. Zehnder, *IEEE Electron Device Lett.* **37**, 269–271 (2016).
9. K. Zhang, M. Sumiya, M. Liao, Y. Koide, L. Sang, *Sci. Rep.* **6**, 23683 (2016).
10. H. Hahn *et al.*, *IEEE Trans. Electron Dev.* **60**, 3005–3011 (2013).
11. B. Reuters *et al.*, *J. Phys. D Appl. Phys.* **47**, 175103 (2014).
12. M. Shatalov *et al.*, *IEEE Electron Device Lett.* **23**, 452–454 (2002).
13. G. Li *et al.*, *IEEE Electron Device Lett.* **34**, 852–854 (2013).
14. A. Nakajima *et al.*, *J. Appl. Phys.* **115**, 153707 (2014).
15. A. Nakajima, Y. Sumida, M. H. Dhyani, H. Kawai, E. M. S. S. Narayanan, *Appl. Phys. Express* **3**, 121004 (2010).
16. Y. Enatsu *et al.*, *Appl. Phys. Express* **9**, 075502 (2016).
17. S. J. Bader *et al.*, *IEEE Electron Device Lett.* **39**, 1848–1851 (2018).
18. S. Birner *et al.*, *IEEE Trans. Electron Dev.* **54**, 2137–2142 (2007).
19. Materials and methods are available as supplementary materials.
20. K. Momma, F. Izumi, *J. Appl. Cryst.* **44**, 1272–1276 (2011).
21. S. J. Bader *et al.*, *Appl. Phys. Lett.* **114**, 253501 (2019).
22. I. P. Smorchkova *et al.*, *J. Appl. Phys.* **86**, 4520–4526 (1999).
23. M. J. Manfra, L. N. Pfeiffer, K. W. West, R. De Picciotto, K. W. Baldwin, *Appl. Phys. Lett.* **86**, 162106 (2005).
24. H. L. Störmer, W. T. Tsang, *Appl. Phys. Lett.* **36**, 685–687 (1980).
25. H. Lee *et al.*, *Nat. Mater.* **17**, 231–236 (2018).
26. T. Yamaguchi *et al.*, *J. Phys. Soc. Jpn.* **82**, 074718 (2013).
27. H. J. Looi, R. B. Jackman, J. S. Foord, *Appl. Phys. Lett.* **72**, 353–355 (1998).
28. K. Hayashi *et al.*, *J. Appl. Phys.* **81**, 744–753 (1997).
29. N. Jiang, T. Ito, *J. Appl. Phys.* **85**, 8267–8273 (1999).
30. M. Kasu, N. Kobayashi, *Appl. Phys. Lett.* **80**, 3961–3963 (2002).
31. M. Myronov, K. Sawano, Y. Shiraki, T. Mouri, K. M. Itoh, *Appl. Phys. Lett.* **91**, 082108 (2007).
32. M. Myronov *et al.*, *Appl. Phys. Lett.* **80**, 3117–3119 (2002).
33. R. J. H. Morris *et al.*, *Semicond. Sci. Technol.* **19**, L106–L109 (2004).
34. H. von Känel *et al.*, *Microelectron. Eng.* **76**, 279–284 (2004).
35. U. König, F. Schaffler, *IEEE Electron Device Lett.* **14**, 205–207 (1993).
36. M. Kaneko, I. Narita, S. Matsumoto, *IEEE Electron Device Lett.* **6**, 575–577 (1985).
37. S. H. Shin, Y. H. Park, H. C. Koo, Y. H. Song, J. D. Song, *Curr. Appl. Phys.* **17**, 1005–1008 (2017).
38. K. Shibata *et al.*, *Appl. Phys. Lett.* **114**, 232102 (2019).
39. M. Karalic *et al.*, *Phys. Rev. B* **99**, 115435 (2019).
40. B. Santic, *Semicond. Sci. Technol.* **18**, 219–224 (2003).
41. S. Nakamura, *Rev. Mod. Phys.* **87**, 1139–1151 (2015).
42. R. Chaudhuri *et al.*, Data for the publication “A polarization-induced 2D hole gas in undoped gallium nitride quantum wells”. Zenodo (2019). doi: 10.5281/zenodo.3245363.

ACKNOWLEDGMENTS

The authors thank V. Protasenko, H. Turski, S. M. Islam, K. Lee, and R. Page for help with the MBE operation and A. Mei and K. Shinohara for assistance with measurements. **Funding:** This

work was supported partly by Intel, the Air Force Office of Scientific Research (AFOSR) (grant AFOSR FA9550-17-1-0048), NSF (grants 1710298 and 1534303), and the Cornell Center for Materials Research, with funding from the NSF Materials Research Science and Engineering Center (MRSEC) program (DMR-1719875). Characterizations and measurements were performed in part at the Cornell NanoScale Facility, a National Nanotechnology Coordinated Infrastructure member supported by NSF (grant ECCS-1542081). The presented data made use of the Cornell Center for Materials Research Shared Facilities, which are supported through the NSF MRSEC program (DMR-1719875) and NSF Major Research Instrumentation (DMR-1429155 and DMR-1338010) programs. Z.C. is funded through PARADIM as part of the NSF Materials Innovation Platform program (DMR-1539918). **Author contributions:** R.C. grew and characterized the samples for the study. S.J.B. supported measurements and performed the numerical simulations. Z.C. performed STEM analysis of the heterostructures, under supervision of D.A.M.; R.C., S.J.B., D.J., and H.X. performed experimental data analysis. R.C. and D.J. wrote the manuscript, with inputs from all authors. **Competing interests:** The authors and Cornell University have filed PCT patent application (PCT/US19/42584) on polarization-induced 2DHG for high voltage p-channel transistors. **Data and materials availability:** All data shown in this work are available at Zenodo (42).

SUPPLEMENTARY MATERIALS

science.sciencemag.org/content/365/6460/1454/suppl/DC1
Materials and Methods
Figs. S1 to S3
Table S1
References (43, 44)

22 July 2018; accepted 3 September 2019
10.1126/science.aau8623

A polarization-induced 2D hole gas in undoped gallium nitride quantum wells

Reet Chaudhuri Samuel James Bader Zhen Chen David A. Muller Huili Grace Xing Debdeep Jena

Science, 365 (6460),

A hole flatland

When two distinct materials are placed on top of each other, the difference in polarization between the two layers can induce charge carriers at the interface. Many such two-dimensional (2D) electron gases have been observed, but engineering a 2D hole gas without the help of doping has been much trickier. Chaudhuri *et al.* used molecular beam epitaxy to grow a layer of gallium nitride on top of aluminum nitride without introducing dopants. This approach resulted in a high-density 2D hole gas at the interface in this technologically relevant system.

Science, this issue p. 1454

View the article online

<https://www.science.org/doi/10.1126/science.aau8623>

Permissions

<https://www.science.org/help/reprints-and-permissions>

Use of this article is subject to the [Terms of service](#)